

# Tunneling Reaction Kinetics for the Hydrogen Abstraction Reaction $\text{H} + \text{H}_2\text{S} \longrightarrow \text{H}_2 + \text{HS}$ in the Interstellar Medium

Thanja Lamberts\* and Johannes Kästner

*Institute for Theoretical Chemistry, University of Stuttgart, Pfaffenwaldring 55, 70569  
Stuttgart, Germany*

E-mail: lamberts@theochem.uni-stuttgart.de

Phone: +49 (0)711 685 64833

## Abstract

The hydrogen abstraction reaction between H and H<sub>2</sub>S, yielding HS and H<sub>2</sub> as products, has been studied within the framework of interstellar surface chemistry. High-temperature rate constants up to 2000 K are calculated in the gas phase and are in agreement with previously reported values. Subsequently low-temperature rate constants down to 55 K are presented for the first time that are of interest to astrochemistry, i.e., covering both bimolecular and unimolecular reaction mechanisms. For this, a so-called implicit surface model is used. Strictly speaking, this is a structural gas-phase model in which the restriction of the rotation in the solid state is taken into account. The calculated kinetic isotope effects are explained in terms of difference in activation and delocalization. All rate constants are calculated at the UCCSD(T)-F12/cc-VTZ-F12 level of theory. Finally, we show that the energetics of the reaction is only affected to a small extent by the presence of H<sub>2</sub>O or H<sub>2</sub>S molecular clusters that simulate an ice surface, calculated at the MPWB1K/def2-TZVP level of theory.

## Introduction

Many interstellar sulfurous compounds have been detected in the gas phase in the past decades<sup>1</sup>. In the ices present in the dark regions of the interstellar medium (ISM), on the other hand, only OCS and tentatively SO<sub>2</sub> are identified<sup>2,3</sup>. Even so, H<sub>2</sub>S has been put forward as a key species in interstellar ice chemistry, and has even been suggested to be responsible for the sulphur depletion in the gas phase in the dense (dark) regions<sup>4-6</sup>. Experimentally, it has been shown that a plethora of surface reactions with H<sub>2</sub>S as a reactant can take place<sup>7-10</sup>. Most of these reactions, however, are induced by energetic processing through which, amongst others, the HS radical is formed. Here, we explore the non-energetic reaction between the hydrogen atom and the hydrogen sulfide molecule:



It is exothermic by about 58 kJ/mol, contrary to the analogous reaction between H and H<sub>2</sub>O which is endothermic by about 62 kJ/mol. Reaction R1 has been proposed to take place as a surface reaction on interstellar ice-covered grains. Indeed it is incorporated specifically in several recent astrochemical surface models that also include the low-temperature regime (10–20 K) in dense molecular clouds<sup>5,11,12</sup>. The two main surface reaction mechanisms are the Langmuir–Hinshelwood (LH) and Eley–Rideal (ER) processes. The LH mechanism assumes two physisorbed reactants that diffuse on the surface, subsequently meet each other, and then form an encounter complex. This encounter complex may decay and lead to a reaction, the rate constant of which is unimolecular. In the ER process on the other hand, a physisorbed species reacts directly with a reactant that impinges from the gas phase. In this case, bimolecular rate constants are required. For a complete understanding of surface astrochemistry, both rate constants are needed.

Furthermore, the title reaction can be of importance in determining the final deuteration fraction of hydrogen sulfide in the ISM. The HDS/H<sub>2</sub>S and D<sub>2</sub>S/H<sub>2</sub>S ratios are brought about via a series of abstraction and addition reactions, listed below, with X = H or D:



In the ISM the HDS/H<sub>2</sub>S ratio has been determined to be 0.1 in the protostar IRAS 16293<sup>13</sup>, and upper limits of  $\sim 10^{-3}$  were found in several hot cores<sup>14</sup>. These, as well as the recently reported cometary value of  $1.2 \times 10^{-3}$  in 67P/Churyumov-Gerasimenko<sup>15</sup> are significantly higher than the cosmic D/H ratio of  $10^{-5}$ <sup>16,17</sup>. This can be seen as a sign that indeed surface

chemistry plays an important role, as outlined by Caselli and Ceccarelli<sup>18</sup>.

Recently, a full-dimensional potential energy surface for the gas-phase reaction has become available with the use of neural networks<sup>19</sup> with which quantum and quasi-classical dynamics studies have been performed subsequently<sup>20</sup>. Although an exchange reaction is in principle also possible, it was found that the abstraction channel is favoured. Within the framework of combustion chemistry, the importance and non-Arrhenius behavior of reaction R1 has been realized<sup>21</sup> and gas-phase rate constants have been both measured and calculated in a temperature range of 200–2560 K<sup>19,22–36</sup>. Non-Arrhenius behavior is a sign of the importance of tunneling for the reaction. The barrier ( $\sim 12.7$  kJ/mol) is indeed quite high to be overcome thermally as the temperature decreases. Since tunneling becomes relatively more important at the low-temperature regime in which we are interested, it has to be taken into account if reaction rate constants are calculated. Note that this also has an effect on the relative rate constants depending if  $X = \text{H}$  or  $\text{D}$  for the reaction sequence R2a–R2f because of the mass-dependency of tunneling.

Here, we are interested primarily in surface reaction rate constants. Therefore we will use the available literature on high-temperature gas-phase rate constants as a reference and subsequently expand the results to low-temperatures in an implicit surface model, elaborate on the isotope effects, and finally show the influence of  $\text{H}_2\text{S}$  and  $\text{H}_2\text{O}$  molecules in the direct vicinity of the reactants. Reaction rate constants are calculated at temperatures down to 55 K with the use of instanton theory that indeed accounts for tunneling inherently. Finally, we will comment on the astrochemical implications and summarize the main findings of this study.

# Computational details

## Electronic structure

The core system is small, 4 atoms and 19 electrons, and can thus be treated well with highly accurate methods. Here, in particular, we made use of (unrestricted) coupled-cluster theory with singles, doubles, and perturbative triple excitations (UCCSD(T))<sup>37–39</sup> and explicitly-correlated geminal functions (UCCSD(T)-F12)<sup>40,41</sup> employing a restricted Hartree–Fock (RHF) reference function and the cc-pVTZ-F12<sup>42</sup> basis set as has been done in the work of Lu and Li<sup>19</sup>. The geometry optimizations are performed using DL-find<sup>43</sup> and Molpro 2012<sup>44</sup> within the Chemshell<sup>45,46</sup> framework.

In order to test the influence of nearby molecules and clusters on the reactivity, we made use of density functional theory (DFT) with Gaussian 09<sup>47</sup>. The functional MPWB1K<sup>48</sup> and basis set def2-TZVP<sup>49</sup> have been employed after comparing the performance to that of single-point energies at the UCCSD(T)-F12/cc-VTZ-F12 level. The purpose of these clusters is to determine the range of activation energies brought about by neighboring molecules, *i.e.*, mimicking a surface. The barrier height, the reaction energy, and four dimer interaction energies have been benchmarked and are listed in Table 1 both excluding zero-point energy (ZPE),  $V$ , and including ZPE,  $E$ . The small energy differences for the activation and interaction energies show that the functional is capable of describing both the cluster structure and the barrier region, both of which are crucial here.

Visual Molecular Dynamics version 1.9.2<sup>50</sup> and Grace version 5.1.23<sup>51</sup> were used for visualization.

## Rate constants

Rate constants have only been calculated for the core system on UCCSD(T)-F12 level with instanton theory<sup>52–55</sup>, *i.e.*, for the four-atomic system. Instanton theory, also known as imaginary- $F$  method or harmonic quantum transition state theory, takes quantum effects of

**Table 1: Comparison of the activation, reaction, and interaction energies in kJ/mol between DFT (MPWB1K/def2-TZVP) and UCCSD(T)-F12/cc-VTZ-F12**

	MPWB1K			UCCSD(T)-F12		
	<i>V</i>	ZPE	<i>E</i>	<i>V</i>	ZPE	<i>E</i>
Activation energy <sup>a</sup>	15.4	-2.4	13.0	15.8	-3.1	12.7
Reaction energy <sup>a</sup>	-49.9	2.6	-47.3	-57.3	2.6	-54.7
Interaction energy H <sub>2</sub> O-H <sub>2</sub> O	-22.9	8.9	-14.0	-21.0 <sup>b</sup>		
Interaction energy H <sub>2</sub> S-H <sub>2</sub> S	-5.8	4.3	-1.5	-6.9 <sup>b</sup>		
Interaction energy H <sub>2</sub> S-H <sub>2</sub> O	-11.8	5.9	-5.9	-11.3 <sup>b</sup>		
Interaction energy H <sub>2</sub> S-H <sub>2</sub> O	-11.9	5.7	-6.2	-12.3 <sup>b</sup>		

<sup>a</sup> with respect to separated reactants

<sup>b</sup> UCCSD(T)-F12 single point energies of geometries calculated at the MPWB1K/def2-TZVP level

atomic movements into account by statistical Feynman path integral theory. Partition functions of both the reactant state and the transition-state-equivalent, the instanton path, are obtained by a steepest-descent approximation to the phase space integrals. The computationally required steps are twofold: (1) The discretized Feynman path has to be optimized to find the instanton, a first-order saddle point in the space of closed Feynman paths. This was performed with a modified Newton–Raphson method.<sup>56,57</sup> (2) The calculation of Hessians of the potential energy at all images of the Feynman path to evaluate the rate constant. For more details on instanton theory we refer to a recent review.<sup>58</sup> Instanton theory is generally considered to be more accurate than one-dimensional tunneling corrections, like Eckart or Bell corrections. Moreover, especially at low temperature it can be expected to be more accurate than small-curvature, large-curvature, or similar tunneling corrections as a result of the temperature-dependent optimization of the tunneling path. The paths were discretized to 60 images and have been calculated between 240 and 55 K. Such a path represents the instanton and is equivalent to the tunneling path with the highest statistical weight. An example is depicted in Fig. 1. It spans the barrier region at temperatures close to the crossover temperature ( $T_c$ , see below) and extends towards the reactant region at low temperature.

The crossover temperature is defined as

$$T_c = \frac{\hbar\omega_b}{2\pi k_B} \quad (1)$$

where  $\omega_b$  is the absolute value of the imaginary frequency at the transition state,  $\hbar$  Planck’s constant divided by  $2\pi$  and  $k_B$  Boltzmann’s constant.  $T_c$  indicates the temperature below which tunneling dominates the reaction.

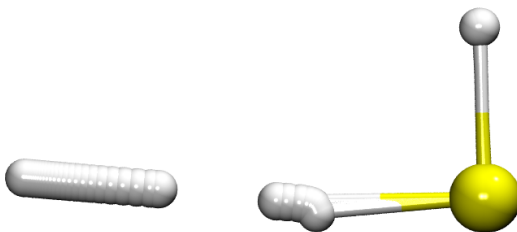


Figure 1: Instanton path calculated at 55 K.

Both bimolecular and unimolecular rate constants have been calculated. The former have been calculated with reduced instanton theory above  $T_c$ <sup>59,60</sup> and with canonical instanton theory below  $T_c$ , choosing parameters equivalently to previous work.<sup>56,57</sup> Convergence is reached when all components of the nuclear gradient are smaller than  $1 \times 10^{-8}$  atomic units. The gradient here is the derivative of the effective energy of the instanton with respect to the mass-weighted atomic coordinates. Rotational and translational partition functions were approximated by their classical analogues (J-shifting approximation). For the reactant partition function in the bimolecular case, the product of the partition functions of the separated reactants was used. For unimolecular cases, the partition function of the encounter complex is employed. Rather than using the available PES<sup>19</sup> we make use of on-the-fly instanton calculations. This choice has been made since Lu and Li<sup>19</sup> state that the coordinates involving the attaching H atom were sampled in relatively sparse grids. We

are, however, also interested in unimolecular rate constants that represent the decay of the encounter complex  $\text{H}\cdots\text{H}_2\text{S}$  for which exactly this part of configuration space would be very important.

For rate constants relevant for surface reactions, several effects of the ice surface need to be taken into account. Thermal equilibrium is assumed at all stages of the calculation and thus excess heat is removed instantaneously. The structural effects are to a certain degree tested with the small cluster study. Finally, the restriction of the rotation of the reactants on a surface must be included as well. This can be mimicked in what is strictly speaking a gas-phase model, through modification of the translational and rotational partition functions. For the unimolecular case, the rotational partition function is assumed to be constant during the reaction, because rotational motions are suppressed in the reactant as well as in the transition state. For bimolecular rate constants, only translation of the H atom is considered, and both rotations and translations of the  $\text{H}_2\text{S}$  molecule are suppressed. This approach is referred to as “implicit surface model”<sup>61</sup>. Only in the gas phase, the full rotational partition function including its symmetry factor<sup>62</sup> is included.

## Results and discussion

### Gas-phase reaction

The calculated vibrationally adiabatic barrier of R1 given in Table 1 amounts to a total of 12.7 kJ/mol with respect to the separated reactants. The crossover temperature is 285 K. Corresponding bimolecular rate constants are depicted in Fig. 2. The high-temperature rate constants coincide with previous experimental and theoretical work<sup>22–36</sup>. With a value of  $1.8\times 10^{-10} \text{ cm}^{-3} \text{ molecule}^{-1} \text{ s}^{-1}$  we are in close agreement with the experimental values of  $\sim 1.5\times 10^{-10} \text{ cm}^{-3} \text{ molecule}^{-1} \text{ s}^{-1}$  at 2000 K, and likewise our value of  $2.3\times 10^{-13} \text{ cm}^{-3} \text{ molecule}^{-1} \text{ s}^{-1}$  is close to the experimental value of  $\sim 2\times 10^{-13} \text{ cm}^{-3} \text{ molecule}^{-1} \text{ s}^{-1}$  at 200 K. Note that these rate constants are calculated using  $\sigma = 2$ . The precise values are listed in



the Supporting Information. The small bump in the curve at 333 K is due to the transition from reduced instanton theory to canonical instanton theory. Finally, the lower end of the temperature range is 70 K, because at even lower temperatures the tunneling energy drops below the total (separated) reactant energy and consequently the calculated rate constant is no longer reliable<sup>63</sup>.

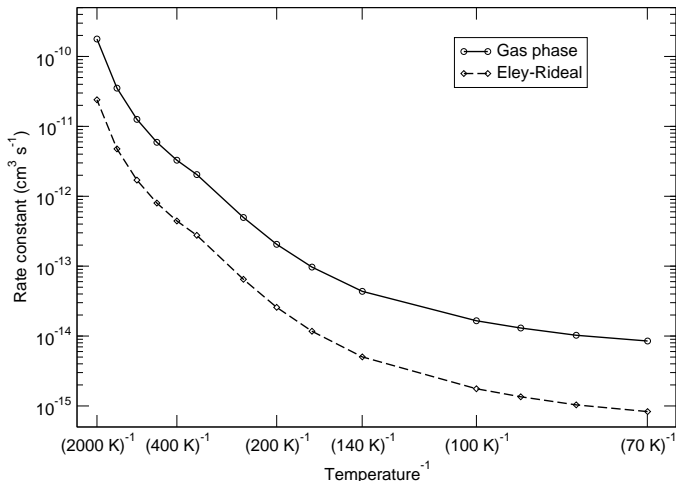


Figure 2: Bimolecular rate constants for the reaction  $\text{H} + \text{H}_2\text{S} \longrightarrow \text{H}_2 + \text{HS}$  in the temperature range of 2000 to 70 K.

Fig. 2 also shows the influence of suppressing reactant rotation. At low temperatures this can lead up to an order of magnitude difference in the rate constant. The values for this bimolecular ER process are given in the Supporting Information. In the following Section the implicit surface model is used for all calculations.

## Isotope effects

The unimolecular rate constants of the decay of the pre-reactive complex  $\text{H}\cdots\text{H}_2\text{S}$  for all eight isotope substitutions are depicted in Fig. 3. The high-temperature behavior can be rationalized using the vibrationally adiabatic activation energies ( $E_{\text{uni, act.}}$ ) summarized in Table 2. The largest rate constants in the high-temperature regime are for those reactions with the lowest barriers. The influence of substituting a protium for a deuterium atom on low-temperature rate constants can be understood from the amount of delocalization of

the respective hydrogen atoms visualized in Fig. 1. Note that the pre-reactive complex is very similar to the image of the path where the H atom is the furthest away from the H<sub>2</sub>S molecule. Other pre-reactive complexes may also be found, *e.g.*, where the incoming H-atom interacts with the S-atom of the H<sub>2</sub>S molecule directly. The difference in the interaction energies is small,  $\sim 0.2$  kJ/mol, and therefore the resulting rate constants are very similar as well. Substituting the incoming atom as well as the one to be abstracted leads to an order of magnitude difference in the rate constant at low temperature, whereas the exchange of the spectator atom has only a vanishing influence.

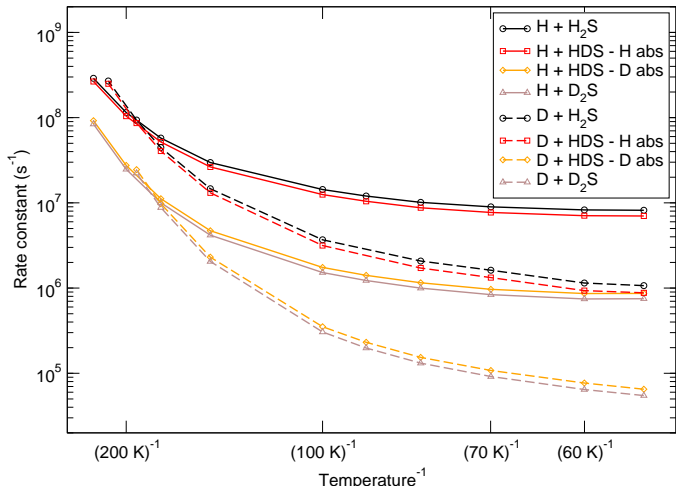


Figure 3: Unimolecular rate constants for the reaction  $\text{H} + \text{H}_2\text{S} \longrightarrow \text{H}_2 + \text{HS}$  and all isotope substitutions in the temperature range of 240 to 55 K.

**Table 2: Unimolecular vibrationally adiabatic barriers and crossover temperatures with respect to the encounter complex**

Reaction	$E_{\text{uni, act.}}$ (kJ/mol)	$T_c$ (K)
$\text{H} + \text{H}_2\text{S} \longrightarrow \text{H}_2 + \text{HS}$	12.6	286
$\text{H} + \text{HDS} \longrightarrow \text{H}_2 + \text{DS}$	12.5	286
$\text{H} + \text{HDS} \longrightarrow \text{HD} + \text{HS}$	15.0	246
$\text{H} + \text{D}_2\text{S} \longrightarrow \text{HD} + \text{DS}$	15.0	246
$\text{D} + \text{H}_2\text{S} \longrightarrow \text{HD} + \text{HS}$	11.3	234
$\text{D} + \text{HDS} \longrightarrow \text{HD} + \text{DS}$	11.2	234
$\text{D} + \text{HDS} \longrightarrow \text{D}_2 + \text{HS}$	13.7	202
$\text{D} + \text{D}_2\text{S} \longrightarrow \text{D}_2 + \text{DS}$	13.7	202

All values for the rate constants are listed in the Supporting Information and can thus

be used in future astrochemical models. For extrapolation to 10 K we propose to use the values at 55 K for the H-addition reactions as the rate constants calculated at 70 K and 55 K are nearly identical. As the D-addition reactions have not yet fully reached an asymptotic value at 55 K, these rate constants can be best seen as upper limits. Unfortunately, it is not possible to calculate rate constants at lower temperatures, because the number of images needs to be increased significantly which increases the computational cost considerably.

## Influence of surface molecules

For the reverse reaction where the sulfur atom is replaced by an oxygen atom,  $\text{H}_2 + \text{OH} \longrightarrow \text{H} + \text{H}_2\text{O}$ , Meisner et al.<sup>61</sup> showed that a water surface had only a very small influence on the reaction. This leads us to believe that there may not be a significant influence of spectator molecules for this reaction as well. To test this hypothesis various water and hydrogen sulfide clusters are constructed to validate the use of the implicit surface model. Table 3 summarizes the difference in activation energy with respect to the encounter complex between the title reaction in the gas phase and on a cluster. These results are calculated fully on the MPWB1K/def2-TZVP level. The differences range between  $-1.8$  and  $+1.2$  kJ/mol with one additional value at 4.1 kJ/mol. In the latter case, the hydrogen atom is oriented such that the distance between the incoming H atom and the closest O-atom is only 2.18 Å. Such an orientation was, however, not obtained in any of the other clusters where the H–O distance amounts to  $\sim 2.7$  Å. Short H–S distances were also found for the  $\text{H}_2\text{S}$  cluster with 5 molecules. The interaction between H and S is, however, not as strong as for the O atom and as such it does not influence the activation energy to a large extent. In conclusion, this approach indeed shows that the influence of neighboring molecules on the reaction is minimal. Therefore, the rate constants calculated within the implicit surface model are a good representation of the average rate constant that may be expected on a surface. The Cartesian coordinates of all transition state structures for the clusters discussed here are given in the Supporting Information along with an image for each structure.

**Table 3: Energy differences in kJ/mol of  $E_{\text{uni, act.}}$  for the title reaction between taking place on a molecular cluster and in the gas phase**

Cluster type	$\Delta E_{\text{act.}}$	Cluster type	$\Delta E_{\text{act.}}$
2 H <sub>2</sub> O A	-0.2	2 H <sub>2</sub> S A	+0.7
2 H <sub>2</sub> O B	+4.1	2 H <sub>2</sub> S B	-1.8
4 H <sub>2</sub> O A	-0.0	5 H <sub>2</sub> S A	-1.5
4 H <sub>2</sub> O B	+1.2	5 H <sub>2</sub> S B	+0.5
5 H <sub>2</sub> O A	-1.6	5 H <sub>2</sub> S C	-1.4
5 H <sub>2</sub> O B	-1.1		

## Conclusion

We have studied the kinetics of the reaction  $\text{H} + \text{H}_2\text{S} \longrightarrow \text{H}_2 + \text{HS}$  with the aim of providing the astrochemical community with accurate rate constants relevant to both gas-phase and surface reactions down to unprecedentedly low temperatures. Therefore, both bi- and unimolecular rate constants are calculated at the UCCSD(T)-F12/cc-VTZ-F12 level, while the main focus lies on surface reactions that take place following a Langmuir-Hinshelwood mechanism. The corresponding kinetic isotope effects are also presented, all within the implicit surface model approximation. The use of this approximation has been validated by investigating the effect of small molecular clusters, up to five molecules, on the energetics of the reaction at the MPWB1K/def2-TZVP level of theory. This has indicated that indeed for the title reaction, the surrounding molecules affect the activation energy only to a small extent. Hence, the rate constants calculated are assumed to be representative for the average value that may be expected for the reaction when it takes place on the surface of an icy interstellar dust grain.

## Acknowledgement

The authors acknowledge support for computer time by the state of Baden-Württemberg through bwHPC and the Germany Research Foundation (DFG) through grant no. INST 40/467-1FUGG. This project was financially supported by the European Union’s Horizon

2020 research and innovation programme (grant agreement No. 646717, TUNNELCHEM). T.L. wishes to acknowledge the Alexander von Humboldt Foundation for generous support. We thank Sonia Álvarez-Barcia, Jan Meisner, Yasuhiro Oba, Takuto Tomaru, and Naoki Watanabe for useful discussions.

## Supporting Information Available

The following files are available free of charge.

- Cluster Geometries : images and coordinates of the various transition state geometries calculated on H<sub>2</sub>O and H<sub>2</sub>S molecular clusters with MPWB1K/def2-TZVP.
- Rate Constants: collection of tables with 1) bimolecular rate constants in the temperature range between 2000 and 70 K calculated with reduced instanton theory above the crossover temperature and with canonical instanton theory below the crossover temperature and 2) unimolecular rate constants in the temperature range 240 to 55 K calculated with canonical instanton theory.

## References

- (1) Molecules in Space. <http://www.astro.uni-koeln.de/cdms/molecules/>, 2017-08-22.
- (2) Palumbo, M. E.; Geballe, T. R.; Tielens, A. G. G. M. Solid Carbonyl Sulfide (OCS) in Dense Molecular Clouds. *Astrophys. J.* **1997**, *479*, 839–844.
- (3) Boogert, A. C. A.; Schutte, W. A.; Helmich, F. P.; Tielens, A. G. G. M.; Wooden, D. H. Infrared observations and laboratory simulations of interstellar CH<sub>4</sub> and SO<sub>2</sub>. *Astron. Astrophys.* **1997**, *317*, 929–941.
- (4) Esplugues, G. B.; Viti, S.; Goicoechea, J. R.; Cernicharo, J., Modelling the sulphur chemistry evolution in Orion KL. *Astron. Astrophys.* **2014**, *567*, A95.

- (5) Holdship, J.; Viti, S.; Jimenez-Serra, I.; Lefloch, B.; Codella, C.; Podio, L.; Benedettini, M.; Fontani, F.; Bachiller, R.; Tafalla, M.; Ceccarelli, C. H<sub>2</sub>S in the L1157-B1 bow shock. *Mon. Not. R. Astron. Soc.* **2016**, *463*, 802–810.
- (6) T. Danilovich and M. Van de Sande and E. De Beck and L. Decin and H. Olofsson and S. Ramstedt and T. J. Millar, Sulphur-bearing molecules in AGB stars I: The occurrence of hydrogen sulfide. *acc. Astron. Astrophys.* **2017**,
- (7) Garozzo, M.,; Fulvio, D.,; Kanuchova, Z.,; Palumbo, M. E.,; Strazzulla, G., The fate of S-bearing species after ion irradiation of interstellar icy grain mantles. *Astron. Astrophys.* **2010**, *509*, A67.
- (8) Jiménez-Escobar, A.,; Muñoz Caro, G. M., Sulfur depletion in dense clouds and circumstellar regions - I. H<sub>2</sub>S ice abundance and UV-photochemical reactions in the H<sub>2</sub>O-matrix. *Astron. Astrophys.* **2011**, *536*, A91.
- (9) Y.-J. Chen and K.-J. Juang and M. Nuevo and A. Jiménez-Escobar and G. M. Muñoz Caro and J.-M. Qiu and C.-C. Chu and T.-S. Yih and C.-Y. R. Wu and H.-S. Fung and W.-H. Ip, Formation of S-bearing Species by VUV/EUV Irradiation of H<sub>2</sub>S-containing Ice Mixtures: Photon Energy and Carbon Source Effects. *Astrophys. J.* **2015**, *798*, 80.
- (10) Z. Kaňuchová and Ph. Boduch and A. Domaracka and M.E. Palumbo and H. Rothard and G. Strazulla , Thermal and energetic processing of astrophysical ice analogues rich in SO<sub>2</sub>. *Astron. Astrophys.* **2017**, *604*, A68.
- (11) Woods, P. M.; Occhiogrosso, A.; Viti, S.; Kaňuchová, Z.; Palumbo, M. E.; Price, S. D. A new study of an old sink of sulphur in hot molecular cores: the sulphur residue. *Mon. Not. R. Astron. Soc.* **2015**, *450*, 1256–1267.
- (12) Vidal, T. H. G.; Loison, J.-C.; Jaziri, A. Y.; Ruaud, M.; Gratier, P.; Wakelam, V. On the reservoir of sulphur in dark clouds: chemistry and elemental abundance reconciled. *Mon. Not. R. Astron. Soc.* **2017**, *469*, 435–447.

- (13) van Dishoeck, E. F.; Blake, G. A.; Jansen, D. J.; Groesbeck, T. D. Molecular Abundances and Low-Mass Star Formation. II. Organic and Deuterated Species toward IRAS 16293-2422. *Astrophys. J.* **1995**, *447*, 760–782.
- (14) Hatchell, J.; Roberts, H.; Millar, T. J. Limits on HDS/H<sub>2</sub>S abundance ratios in hot molecular cores. *Astron. Astrophys.* **1999**, *346*, 227–232.
- (15) Altwegg, K.; Balsiger, H.; Berthelier, J. J.; Bieler, A.; Calmonte, U.; De Keyser, J.; Fiethe, B.; Fuselier, S. A.; Gasc, S.; Gombosi, T. I.; Owen, T.; Le Roy, L.; Rubin, M.; Sémon, T.; Tzou, C.-Y. D<sub>2</sub>O and HDS in the coma of 67P/Churyumov–Gerasimenko. *Phil. Trans. R. Soc. A* **2017**, *375*.
- (16) Piskunov, N.; Wood, B. E.; Linsky, J. L.; Demfsey, R. C.; Ayres, R. Local Interstellar Medium Properties and Deuterium Abundances for the Lines of Sight toward HR 1099, 31 Comae,  $\beta$  Ceti, and  $\beta$  Cassiopeiae. *Astrophys. J.* **1997**, *474*, 315–328.
- (17) Oliveira, C. M.; Hébrard, G.; Howk, J. C.; Kruk, J. W.; Chayer, P.; Moos, H. W. Interstellar Deuterium, Nitrogen, and Oxygen Abundances toward GD 246, WD 2331-475, HZ 21, and Lanning 23: Results from the FUSE Mission. *Astrophys. J.* **2003**, *587*, 235–255.
- (18) Caselli, P.; Ceccarelli, C. Our astrochemical heritage. *Astron. Astrophys. Rev.* **2012**, *20*, 56.
- (19) Lu, D.; Li, J. Full-dimensional global potential energy surface describing abstraction and exchange for the H + H<sub>2</sub>S reaction. *J. Chem. Phys.* **2016**, *145*, 014303 1–10.
- (20) Qi, J.; Lu, D.; Song, H.; Li, J.; Yang, M. Quantum and quasiclassical dynamics of the multi-channel H + H<sub>2</sub>S reaction. *J. Chem. Phys.* **2017**, *146*, 124303 1–8.
- (21) Hynes, A. J.; Wine, P. H. In *Gas-Phase Combustion Chemistry*; Gardiner, W. C., Ed.; Springer New York: New York, NY, 2000; pp 343–388.

- (22) Cupitt, L. T.; Glass, G. P. Reaction of atomic oxygen with hydrogen sulphide. *Trans. Faraday Soc.* **1970**, *66*, 3007–3015.
- (23) Kurylo, M. J.; Peterson, N. C.; Braun, W. Absolute Rate of the Reaction  $\text{H} + \text{H}_2\text{S}$ . *J. Chem. Phys.* **1971**, *54*, 943–946.
- (24) Rommel, H.; Schiff, H. I. The Reactions of H Atoms with  $\text{H}_2\text{S}$  and  $\text{COS}$ . *Int. J. Chem. Kin.* **1972**, *4*, 547–558.
- (25) Bradley, J. N.; Trueman, S. P.; Whytock, D. A.; Zaleski, T. A. Electron spin resonance study of the reaction of hydrogen atoms with hydrogen sulphide. *J. Chem. Soc., Faraday Trans. 1* **1973**, *69*, 416–425.
- (26) Pratt, G.; Rogers, D. Homogeneous isotope exchange reactions. Part 3.- $\text{H}_2\text{S} + \text{D}_2$ . *J. Chem. Soc., Faraday Trans. 1* **1977**, *73*, 54–61.
- (27) Wojciechowski, K.; Baj, H.; Forys, M. Vacuum ultraviolet photolysis of hydrogen sulphide. *J. Chem. Soc., Faraday Trans. 2* **1979**, *75*, 1085–1094.
- (28) Nicholas, J. E.; Amodio, C. A.; Baker, M. J. Kinetics and mechanism of the decomposition of  $\text{H}_2\text{S}$ ,  $\text{CH}_3\text{SH}$  and  $(\text{CH}_3)_2\text{S}$  in a radio-frequency pulse discharge. *J. Chem. Soc., Faraday Trans. 1* **1979**, *75*, 1868–1875.
- (29) Husain, D.; Slater, N. K. H. Kinetic study of the reactions of hydrogen and deuterium atoms with  $\text{HBr}$  and  $\text{DBr}$  by time-resolved resonance fluorescence. *J. Chem. Soc., Faraday Trans. 2* **1980**, *76*, 276–285.
- (30) Roth, P.; Löhr, R.; Barner, U. Thermal decomposition of hydrogen sulfide at low concentrations. *Combust. Flame* **1982**, *45*, 273–285.
- (31) Clyne, M. A.; Ono, Y. Determination of the rate constant of reaction of ground-state  $\text{Cl}$  and  $\text{H}$  atoms with  $\text{H}_2\text{S}$  using resonance fluorescence in a discharge flow. *Chem. Phys. Lett.* **1983**, *94*, 597–602.



- (32) Yoshimura, M.; Koshi, M.; Matsui, H.; Kamiya, K.; Umeyama, H. Non-Arrhenius temperature dependence of the rate constant for the  $\text{H} + \text{H}_2\text{S}$  reaction. *Chem. Phys. Lett.* **1992**, *189*, 199–204.
- (33) Peng, J.; Hu, X.; Marshall, P. Experimental and ab Initio Investigations of the Kinetics of the Reaction of H Atoms with  $\text{H}_2\text{S}$ . *J. Phys. Chem. A* **1999**, *103*, 5307–5311.
- (34) Kurosaki, Y.; Takayanagi, T. Theoretical study of the non-Arrhenius temperature dependence of thermal rate constants for the  $\text{H} + \text{H}_2\text{S} \longrightarrow \text{H}_2 + \text{SH}$  reaction. *J. Chem. Phys.* **1999**, *111*, 10529–10536.
- (35) Huang, C.-H.; You, R.-M.; Lian, P.-Y.; Hu, W.-P. Improved Interpolated Correction Schemes for Dual-Level Direct Dynamics Calculation. *J. Phys. Chem. A* **2000**, *104*, 7200–7208.
- (36) Vandeputte, A. G.; Reyniers, M.-F.; Marin, G. B. A theoretical study of the thermodynamics and kinetics of small organosulfur compounds. *Theor. Chem. Acc.* **2009**, *123*, 391–412.
- (37) Knowles, P. J.; Hampel, C.; Werner, H.-J. Coupled cluster theory for high spin, open shell reference wave functions. *J. Chem. Phys.* **1993**, *99*, 5219–5227.
- (38) Knowles, P. J.; Hampel, C.; Werner, H.-J. Erratum: “Coupled cluster theory for high spin, open shell reference wave functions” [ *J. Chem. Phys.* *99*, 5219 (1993)]. *J. Chem. Phys.* **2000**, *112*, 3106–3107.
- (39) Deegan, M. J. O.; Knowles, P. J. Perturbative corrections to account for triple excitations in closed and open-shell coupled-cluster theories. *Chem. Phys. Lett.* **1994**, *227*, 321–326.
- (40) Adler, T. B.; Knizia, G.; Werner, H.-J. A simple and efficient CCSD(T)-F12 approximation. *J. Chem. Phys.* **2007**, *127*, 221106.

- (41) Knizia, G.; Adler, T. B.; Werner, H.-J. Simplified CCSD(T)-F12 methods: Theory and benchmarks. *J. Chem. Phys.* **2009**, *130*, 054104.
- (42) Peterson, K. A.; Adler, T. B.; Werner, H.-J. Systematically convergent basis sets for explicitly correlated wavefunctions: The atoms H, He, B-Ne, and Al-Ar. *J. Chem. Phys.* **2008**, *128*, 084102.
- (43) Kästner, J.; Carr, J. M.; Keal, T. W.; Thiel, W.; Wander, A.; Sherwood, P. DL-FIND: An Open-Source Geometry Optimizer for Atomistic Simulations. *J. Phys. Chem. A* **2009**, *113*, 11856–11865.
- (44) Werner, H.-J. et al. MOLPRO, version 2015.1, a package of ab initio programs. 2015; see <http://www.molpro.net>.
- (45) Sherwood, P. et al. QUASI: A general purpose implementation of the QM/MM approach and its application to problems in catalysis. *J. Mol. Struct. (THEOCHEM)* **2003**, *632*, 1–28.
- (46) Metz, S.; Kästner, J.; Sokol, A. A.; Keal, T. W.; Sherwood, P. ChemShell—a modular software package for QM/MM simulations. *WIREs Comput. Mol. Sci.* **2014**, *4*, 101–110.
- (47) Frisch, M. J. et al. Gaussian 09 Revision D.01. Gaussian Inc. Wallingford CT 2016.
- (48) Zhao, Y.; Truhlar, D. G. Hybrid Meta Density Functional Theory Methods for Thermochemistry, Thermochemical Kinetics, and Noncovalent Interactions: The MPW1B95 and MPWB1K Models and Comparative Assessments for Hydrogen Bonding and van der Waals Interactions. *J. Chem. Phys. A* **2004**, *108*, 6908–6918.
- (49) Weigend, F.; Häser, M.; Patzelt, H.; Ahlrichs, R. RI-MP2: optimized auxiliary basis sets and demonstration of efficiency. *Chem. Phys. Lett.* **1998**, *294*, 143–152.

- (50) Humphrey, W.; Dalke, A.; Schulten, K. VMD: Visual molecular dynamics. *J. Mol. Graph.* **1996**, *14*, 33–38.
- (51) Grace. <http://plasma-gate.weizmann.ac.il/Grace/>.
- (52) Langer, J. Theory of the condensation point. *Ann. Phys.* **1967**, *41*, 108–157.
- (53) Miller, W. H. Semiclassical limit of quantum mechanical transition state theory for nonseparable systems. *J. Chem. Phys.* **1975**, *62*, 1899–1906.
- (54) Callan, C. G.; Coleman, S. Fate of the false vacuum. II. First quantum corrections. *Phys. Rev. D* **1977**, *16*, 1762–1768.
- (55) Coleman, S. Fate of the false vacuum: Semiclassical theory. *Phys. Rev. D* **1977**, *15*, 2929–2936.
- (56) Rommel, J. B.; Goumans, T. P. M.; Kästner, J. Locating Instantons in Many Degrees of Freedom. *J. Chem. Theory Comput.* **2011**, *7*, 690–698.
- (57) Rommel, J. B.; Kästner, J. Adaptive integration grids in instanton theory improve the numerical accuracy at low temperature. *J. Chem. Phys.* **2011**, *134*, 184107.
- (58) Kästner, J. Theory and Simulation of Atom Tunneling in Chemical Reactions. *WIREs Comput. Mol. Sci.* **2014**, *4*, 158–168.
- (59) Kryvohuz, M. Semiclassical instanton approach to calculation of reaction rate constants in multidimensional chemical systems. *J. Chem. Phys.* **2011**, *134*, 114103.
- (60) McConnell, S.; Kästner, J. Instanton rate constant calculations close to and above the crossover temperature. *J. Comp. Chem.* **2017**, *38*, 2570–2580.
- (61) Meisner, J.; Lamberts, T.; Kästner, J. Atom Tunneling in the Water Formation Reaction  $\text{H}_2 + \text{OH} \rightarrow \text{H}_2\text{O} + \text{H}$  on an Ice Surface. *ACS Earth Space Chem.* **2017**, *1*, 399–410.

- (62) Fernández-Ramos, A.; Ellingson, B. A.; Meana-Pañeda, R.; Marques, J. M. C.; Truhlar, D. G. Symmetry numbers and chemical reaction rates. *Theor. Chem. Acc.* **2007**, *118*, 813–826.
- (63) McConnell, S. R.; Löhle, A.; Kästner, J. Rate constants from instanton theory via a microcanonical approach. *J. Chem. Phys.* **2017**, *146*, 074105.

## Graphical TOC Entry

